

Optical Power Control Strategies for Optimized C+L+S-bands Network Performance

*Original*

Optical Power Control Strategies for Optimized C+L+S-bands Network Performance / Correia, Bruno; Sadeghi, Rasoul; Virgillito, Emanuele; Napoli, Antonio; Costa, Nelson; Pedro, João; Curri, Vittorio. - ELETTRONICO. - (2021), pp. 1-3. ((Intervento presentato al convegno OFC tenutosi a Washington, DC United States nel 6–11 June 2021.

*Availability:*

This version is available at: 11583/2933953 since: 2021-11-23T10:47:11Z

*Publisher:*

Optica Publishing Group

*Published*

DOI:

*Terms of use:*

openAccess

This article is made available under terms and conditions as specified in the corresponding bibliographic description in the repository

*Publisher copyright*

Optica Publishing Group (formely OSA) postprint/Author's Accepted Manuscript

“© 2021 Optica Publishing Group. One print or electronic copy may be made for personal use only. Systematic reproduction and distribution, duplication of any material in this paper for a fee or for commercial purposes, or modifications of the content of this paper are prohibited.”

(Article begins on next page)

# Optical Power Control Strategies for Optimized C+L+S-bands Network Performance

Bruno Correia<sup>1</sup>, Rasoul Sadeghi<sup>1</sup>, Emanuele Virgillito<sup>1</sup>, Antonio Napoli<sup>2</sup>, Nelson Costa<sup>3</sup>, João Pedro<sup>3,4</sup>, Vittorio Curri<sup>1</sup>

<sup>1</sup> DET, Politecnico di Torino, C.so Duca degli Abruzzi 24, 10129 Torino, Italy

<sup>2</sup> Infinera, St.-Martin-Straße 76, 81541 Munich, Germany

<sup>3</sup> Infinera Unipessoal Lda, Rua da Garagem 1, 2790-078 Carnaxide, Portugal

<sup>4</sup> Instituto de Telecomunicações, Instituto Superior Técnico, Avenida Rovisco Pais 1, 1049-001 Lisboa, Portugal  
bruno.dearaujo@polito.it

**Abstract:** This work describes and assesses the performance of a meta-heuristic algorithm applied for launch power control in multi-band (C+L+S) optical networks. © 2021 The Author(s)

## 1. Introduction

The imminent 5G deployment [1] and the increasing IP data traffic will require more and more capacity from backbone optical networks, stressing them and demanding additional investments to unlock more capacity. To increase the network throughput, band-division multiplexing (BDM) has been proposed [2]. This solution aims to exploit, in addition to the C-band, the entire low loss fiber bandwidth, which comprises  $\sim 50$  THz in modern standard single-mode fibers (SSMF) [2], significantly reducing the upgrade costs when compared to, for example, using parallel fibers. In such scenario, the most relevant effect is the stimulated Raman scattering (SRS) [3], producing an energy transfer from higher to lower frequencies – between channels – during fiber propagation [4] and an interaction with the nonlinear interference (NLI) noise generation. Together with the NLI, the amplified spontaneous emission (ASE) noise produced by optical amplifiers can be used to compute the quality of transmission (QoT) metric called generalized signal-to-noise ratio (GSNR) [5]. Due to the SRS, amplifiers need to apply a non-flat gain, resulting in a GSNR tilting. Another factor that impacts the QoT in wideband systems is the different types of amplifiers for transmission beyond C- and L-band, which are still being developed [6]. Consequently, the noise-figure (NF) is not completely flat, resulting in a frequency-dependent contribution to the ASE noise and consequently an impact on GSNR. Attaining a GSNR that is (i) high and (2) as much as possible flat, becomes a critical aspect to be taken into account by the network controller: the former enables to choose more spectrally efficient modulation formats, while the latter reduces the complexity of the routing, modulation, and wavelength assignment (RMSA). To cope with these requirements, one possible strategy is the usage of an input power as a pre-tilting and offset for each spectral band, starting from local-optimization global-optimization (LOGO) [7] flat launch power. This strategy, applied in previous works for BDM with C+L-band transmission [8] using an Exhaustive Search (ES) approach, consists in controlling the launch power of each spectrum band individually in terms of offset (in dB) and pre-tilt (in dB/THz) to compensate for the GSNR tilting [3].

This work proposes two methods to use the pre-tilting and offset strategy in a C+L+S-band scenario. The first method consists in dividing the S-band into several sub-bands and apply independent values of pre-tilting and offset using the Exhaustive Search (ES) procedure. This division is related to the possible difficulty to find a single value for tilt and one for offset that can deal with the higher attenuation coefficients as well as the different values of NF along this band. The second approach applies a multi-objective genetic algorithm (GA) [9] to find the best value of pre-tilt and offset, without sub-dividing the S-band. We show that the latter approach, not only uses a single value pair for the entire S-band and reduces the computational effort, but is also able to maintain high GSNR average levels and significantly increase the GSNR flatness. Besides quality-of-transmission (QoT) evaluation, we compare the BDM upgrade with spatial-division multiplexing (SDM) using multi-parallel fibers, with the same total number of channels in a network scenario. It is shown that BDM enables to increase the total allocated traffic (using C+L+S-band instead of multi-parallel C-band) more than  $\times 4$  times and presents a comparable performance with respect to the SDM upgrade.

## 2. QoT Evaluation and Optimization Algorithms

The optical line system is assumed to be composed of equal spans of 75 km with ITU-T G.652D fiber. C- and L-band are amplified by two separated erbium-doped fiber amplifiers (EDFAs) and S-band by a thulium-doped fiber amplifier (TDFA) prototype [11], which have an average NF of [6.5, 4.25, 4.68] dB for S-, C-, L-band, respectively. Complete fiber loss compensation by the amplifiers is considered, i.e., in-line amplifiers are set to the typical operation at a gain defined by the controller. C- and L-band are filled in with up to 96 channels each, and S-band with up to 192 channels on the ITU-T 50 GHz spectrum grid, assuming a channel symbol rate of 32 Gbaud. Moreover, a guard band of 500 GHz is considered between each band. The LOGO powers per channel,

which are used as a reference case for the power optimization are [-1.99, -2.11, -2.06] dBm for L-, C- and S-band, respectively. The NLI contribution is computed for 5 channels in the bands with 96 channels and 10 channels from 192 channels of S-band with about 1 THz of spacing between them.

In [8] the optimization based on ES has been performed for the C- and L-band, with pre-tilt and offset values being set to [0.5 dB/THz, -1.0 dB] for the C-band and [-0.5 dB/THz, -1.0 dB] for the L-band. In the next step the S-band is (virtually) divided in 4 independent sub-bands with 48 channels each and different combinations of power settings are performed. To be more precise, for each sub-band the pre-tilt range considered is between -0.5 and 0.5 dB/THz (with a step of 0.5 dB/THz) and the offset range considered varies from 0.0 to 2.0 dB (with a step of 1.0 dB). This results in a total of 6560 combinations that have to be evaluated. The best combination regarding GSNR average and flatness is chosen. The GA-based optimization is done using the NSGA-II [9] framework targeting GSNR average and flatness. Each chromosome represents a value (pre-tilt or offset) for each spectral band. The algorithm performs a total of 60 iterations with a population size of 60 individuals (3660 evaluations in total). The probability of crossover and mutation is 0.9 and  $1/n$ , respectively, in which  $n$  is the number of chromosomes of each individual. From the last iteration, we retrieve a solution from the Pareto front in order to compare with the ES approach. It is worth mentioning that the flatness is computed in terms of  $\Delta$ GSNR, which means the total average of difference between the maximum and minimum GSNR in each band. Therefore, the objective is to maximize the average GSNR, while minimizing the  $\Delta$ GSNR.

Finally, a network assessment is performed by the Statistical Network Assessment Process (SNAP) framework [10], which runs Monte-Carlo simulations to extract meaningful network-wide statistics. The German topology, which comprises 17 ROADM nodes and 26 links, is considered. The aim is to compare the BDM upgrade network capacity versus blocking probability (BP) with that obtained with SDM upgrade, assuming the same overall number of channels (384) for both upgrade strategies. We considered 30000 Monte-Carlo iterations, a progressive-traffic analysis with uniform traffic distribution,  $k$ -shortest path as a routing algorithm, with  $k_{max} = 15$ , and best GSNR wavelength assignment policy. The traffic of each allocated lightpath is evaluated, assuming perfectly elastic transceivers, according to the Shannon limit, thereby avoiding to consider the limitations of specific transceiver technology and focusing instead on the transmission limitations.

### 3. Results

The GA evolution is presented in Fig. 1(a), showing the initial population and the Pareto front for several iterations, in terms of GSNR average versus  $\Delta$ GSNR. It can be noticed that after a small number of iterations, the algorithm is able to find solutions with high average and flatness (left corner), with the last iterations (zoomed plot) serving to diversify the population, i.e., increase the number of non-dominated solutions.

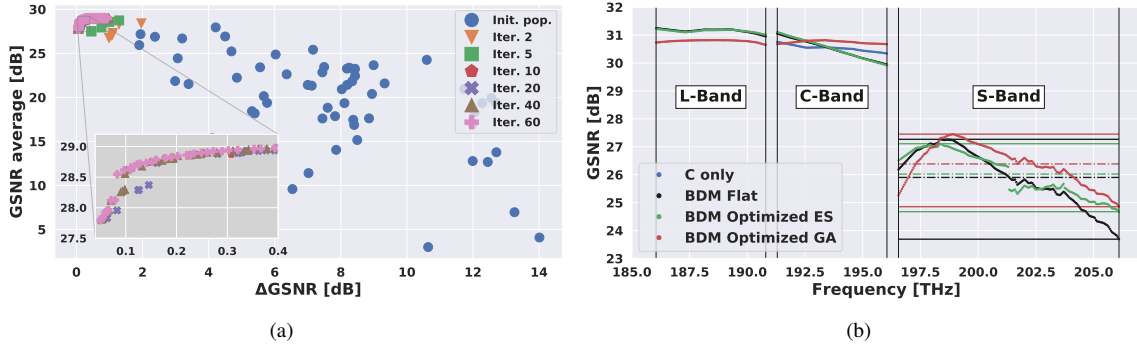


Fig. 1. (a) Genetic algorithm evolution in terms of  $\Delta$ GSNR and average and (b) GSNR profiles for all scenarios analysed.

With a particular solution selected from the last Pareto front obtained in GA strategy and with the best solution found by the ES strategy, we compare them with the S-band without any compensation and plot the results in Fig. 1(b). We also present the GSNR profile for the C-band only case (blue line), also optimized using the ES approach. Firstly, it is possible to see that the GA strategy (red lines) is able to delivery an almost flat GSNR profile for C- and L-band and increase the C-band average, compared with the C-band only case, with the GSNR average for L-band being decreased. The decrease observed in L-band is compensated by an increase of the GSNR average in the S-band (dashed line) while significantly improving the GSNR flatness in this band (maximum and minimum values as solid lines), compared with a profile without pre-tilt and offset in the same band (black lines). Regarding the ES strategy (green lines), the best profile found increases the flatness in S-band (solid lines), compared with BDM Flat, while slightly increasing the GSNR average (dashed line). The quantitative analysis regarding the average and flatness per band of each scenario is summarized in Table 1. When using the GA, it results in a  $\Delta$ GSNR of 0.2, 0.1 and 2.6 dB and average of 30.8, 30.7 and 26.4 dB, for L-, C- and S-band, respectively. For the ES strategy, the figures are 0.3, 1.2 and 2.4 dB in flatness, and 31.1, 30.5 and 25.9 dB in average for L-, C-

and S-band, respectively. Overall, the GA strategy shows a better performance with a fixed number of iterations. As usually GA uses a fixed number of iterations and population size, this algorithm could work with a scenarios with more spectral bands together with bands sub-division, as used by the ES strategy, without increasing the total number of evaluations performed.

Table 1.  $\Delta$ GSNR and GSNR average per spectral band for all scenarios analyzed.

Scenarios		Spectral bands		
		L	C	S
C-band only	Avr.	-	30.5	-
	$\Delta$ GSNR	-	0.4	-
BDM S-band flat	Avr.	31.1	30.5	25.9
	$\Delta$ GSNR	0.3	1.1	3.6
BDM Optimized ES	Avr.	31.1	30.5	25.9
	$\Delta$ GSNR	0.3	1.2	2.4
BDM Optimized GA	Avr.	30.8	30.7	26.4
	$\Delta$ GSNR	0.2	0.1	2.6

Finally, Fig. 3 shows the results of the network assessment, comparing the performance of BDM-C+L+S (using the GA strategy GSNR profile) versus SDM (C-band only GSNR profile). In order to perform a fair comparison, both techniques consider a total of 384 channels, which means that SDM assumes 4 fiber pairs per link with 96 channels each. Fig. 2(a) shows the total allocated traffic versus BP, with BP varying from  $10^{-4}$  to  $10^{-1}$ . It can be noticed that the difference is almost constant for the entire range of traffic loads tested. The larger difference is at  $BP=10^{-1}$ , with BDM delivering 1284 Tbps and SDM delivering 1337 Tbps in total. For  $BP=10^{-2}$ , we also present the traffic upgrade multiplicative factor in Fig. 2(b), having as benchmark for both techniques the C-band single fiber pair case. BDM increases the allocated traffic by 4.28 times (1150 Tbps) while SDM increases it by 4.43 times (1188 Tbps). Even with BDM upgrade presenting a worst performance, it is comparable with SDM in terms of delivered traffic, showing that the BDM solution together with adopting an accurate multi-band power control strategy is a solid alternative to provide better QoT and multiply the network capacity without having to install or lease new fibers.

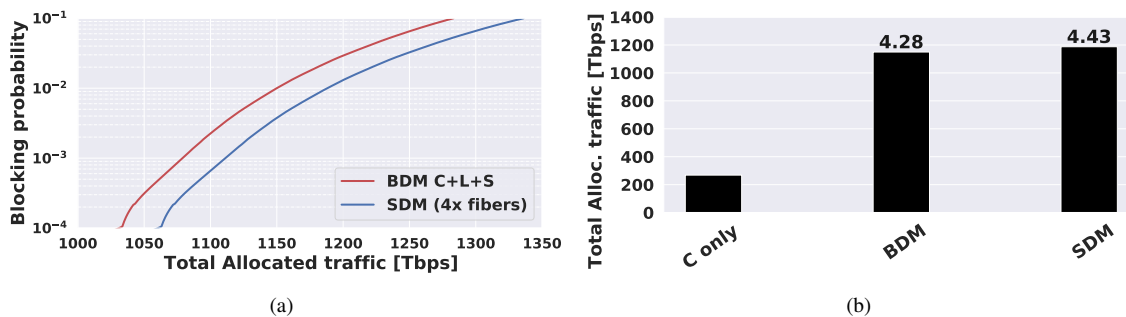


Fig. 2. (a) Total allocated traffic versus BP with BDM and SDM upgrades and (b) allocated traffic multiplicative factor for BDM and SDM comparing with C-band only scenario.

#### 4. Conclusion

We show that the use of a meta-heuristic optimization algorithm applied to the tilt and offset strategy in launch power control can be used to provide better QoT performance, reducing the total GSNR tilting by 2 dB and increasing the total average GSNR by  $\sim 0.5$  dB, when compared to the case without tilt and offset compensation. We further showed that the network capacity upgrade provided by BDM more than quadruples the total allocated traffic, performing very close to a SDM upgrade that demands using 4 times the amount of fibers.

#### Acknowledgment

This work was partially funded by the EU H2020 within the ETN WON, grant agreement 814276 and by the Telecom Infra Project.

#### References

1. P. Ohlen et al., JLT, vol. 34, no. 6, pp. 1501-1508, 2016.
2. A. Ferrari et al., JLT, vol. 38, no. 16, pp. 4279-4291, 2020.
3. A. Ferrari et al., OFC, 2019, pp. 10-12, OSA, 2019.
4. M. Cantono et al., JLT, vol. 38, no. 5, pp. 1050-1060, 2020.
5. V. Curri, ICTON, 2020, p. We.C2.1, IEEE
6. A. Napoli et al., Advanced Photonics, pp. NeTu3E.1, Part F106-, 2018.
7. V. Curri et al., JLT, pp. 3921-3932, no. 18, vol. 33, sep. 2015.
8. E. Virgillito et al., OFC 2020, pp. M2G.4, 2020.
9. K. Deb et al., IEEE Trans. Evol. Comput., pp. 182-197, no. 2, vol. 6, 2002.
10. V. Curri et al., JLT, pp. 1211-1221, no. 6, vol. 35, 2017.
11. AMP-FL8221-SB-16 Amplifier Datasheet from Fiber-Labs Inc.